Journal of Theoretical Biology 265 (2010) 467–480

Contents lists available at ScienceDirect

Journal of Theoretical Biology

journal homepage: www.elsevier.com/locate/yjtbi

Modeling anti-tumor Th1 and Th2 immunity in the rejection of melanoma

Raluca Eftimie [a,*], Jonathan L. Bramson [b,c], David J.D. Earn [a,c]

[a] Department of Mathematics and Statistics, McMaster University, Hamilton, ON, Canada L8S 4K1
[b] Centre for Gene Therapeutics, Department of Pathology and Molecular Medicine, McMaster University, Hamilton, ON, Canada L8N 3Z5
[c] Michael G. DeGroote Institute for Infectious Disease Research, McMaster University, Hamilton, ON, Canada L8N 4L8

ARTICLE INFO

Article history:
Received 27 November 2009
Received in revised form
21 April 2010
Accepted 30 April 2010
Available online 5 May 2010

Keywords:
Cancer immunology
Mathematical modeling
$CD4^+$ T cells
Granulocytes
Melanoma

ABSTRACT

Recent experiments indicate that $CD4^+$ Th2 cells can reject skin tumors in mice, while $CD4^+$ Th1 cells cannot (Mattes et al., 2003; Zhang et al., 2009). These results are surprising because $CD4^+$ Th1 cells are typically considered to be capable of tumor rejection. We used mathematical models to investigate this unexpected outcome. We found that neither $CD4^+$ Th1 nor $CD4^+$ Th2 cells could eliminate the cancer cells when acting alone, but that tumor elimination could be induced by recruitment of eosinophils by the Th2 cells. These recruited eosinophils had unexpected indirect effects on the decay rate of type 2 cytokines and the rate at which Th2 cells are inactivated through interactions with cancer cells. Strikingly, the presence of eosinophils impacted tumor growth more significantly than the release of tumor-suppressing cytokines such as IFN-γ and TNF-α. Our simulations suggest that novel strategies to enhance eosinophil recruitment into skin tumors may improve cancer immunotherapies.

1. Introduction

T lymphocytes play a critical role in controlling cancer (Shankaran et al., 2001; Smyth et al., 2001). These lymphocytes can be divided into two major classes: (1) $CD8^+$ T cells, which typically reject tumors by direct interaction with targets on the tumor cell, and (2) $CD4^+$ T cells, which typically reject tumors through indirect means following stimulation by other immune cells infiltrating the tumor, such as antigen presenting cells (APCs). $CD8^+$ T cells were initially thought to be the principal effectors in anti-tumor immunity due to their ability to directly lyse tumor cells, whereas $CD4^+$ T cells were thought to play only a supportive role in $CD8^+$ T cell activation (Behrens et al., 2004). However, there is increasing evidence supporting a direct role for $CD4^+$ T cells in anti-tumor immunity, independent of $CD8^+$ T cells (Hung et al., 1998; Toes et al., 1999; Zeng, 2001; Corthay et al., 2005; Perez-Diez et al., 2007; Lane et al., 2004; Leitch et al., 2004; Wan et al., 2000).

Although the exact mechanisms by which $CD4^+$ T cells eliminate cancer cells is not fully elucidated, there is evidence that they do so via the secretion of tumor-suppressive cytokines and activation of innate effectors, such as granulocytes, which can exert direct tumoricidal functions (Mattes et al., 2003). Tumors can evade $CD8^+$ T cell attack by losing or down-regulating their surface major histocompatibility complex molecules (MHC) (Algarra et al., 2000; Garcia-Lorca et al., 2003). Remarkably, the indirect nature of $CD4^+$ T cell-mediated tumor rejection overcomes this mechanism. In fact, several reports have demonstrated that $CD4^+$ T cells can eliminate MHC-negative tumors which are resistant to $CD8^+$ T cells (Perez-Diez et al., 2007; Wan et al., 2000; Ossendorp et al., 1998; Qin and Blankenstein, 2000).

Given the utility of $CD4^+$ T cell responses for cancer immunotherapy, in this article we focus on the effector role of these T cells. Following emergence from the thymus, antigen-specific $CD4^+$T cells exist in a naïve state with limited functional capacity. Upon encounter with antigen, signals from antigen presenting cells and the microenvironment of the lymph node (where the $CD4^+$ T cells encounter the antigen presenting cells) promote proliferation of the naïve cells and differentiation of the daughter cells. Historically, differentiated $CD4^+$ T cell effectors were separated into two categories, Th1 and Th2, which were defined by the cytokines produced by the T cells upon stimulation. Th1 cells secrete pro-inflammatory cytokines, such as IFN-γ, whereas Th2 cells produce anti-inflammatory cytokines, such as IL-4, IL-5, and IL-13. Both Th1 and Th2 cells have the potential to cause damage to the tumor microenvironment through the release of cytokines that suppress angiogenesis (growth of new blood vessels from pre-existing vessels) and act as chemoattractants for tumoricidal cells such as NK cells, macrophages and granulocytes (Hung et al., 1998; Qin and Blankenstein, 2000; Mattes et al., 2003; Volpert et al., 1998).

In this article, we investigate the surprising observation that Th2 cells, but not Th1 cells, are responsible for rejecting skin tumors produced by the widely used B16F10 melanoma cell line that grows in immune-competent mice (Mattes et al., 2003; Zhang et al., 2009). As a tool to make sense of these observed tumor–immune interactions, we used mathematical models.

Many types of models have been employed to identify mechanisms that could explain observed cancer-immune system

* Corresponding author. Tel.: +1 905 525 9140x26056; fax: +1 905 522 0935.
E-mail address: reftimie@math.mcmaster.ca (R. Eftimie).

0022-5193/$ - see front matter © 2010 Elsevier Ltd. All rights reserved.
doi:10.1016/j.jtbi.2010.04.030

interactions (see, for example, Araujo and McElwain, 2004; Bellomo and Preziosi, 2000; Bellomo et al., 2008; Byrne et al., 2006; Martins and Vilela, 2007; Nagy, 2005; Roose et al., 2007; Chaplain, 2008; Eftimie et al., 2010, and the references therein). The majority of these models focus on spatial processes, which are described either by partial differential equations (PDE) or cellular automata (CA) (e.g., Chaplain et al., 1998; Araujo and McElwain, 2004; Roose et al., 2007; Chaplain, 2008; Matzavinos and Chaplain, 2004; Matzavinos et al., 2004; Owen and Sherratt, 1997, 1999). Another class of models of tumor–immune interactions is based on the mathematical kinetic theory of "active particles", which gives a statistical description of the evolution of large populations of cells that undergo kinetic interactions (see, for example, Bellomo and Preziosi, 2000; Bellomo et al., 2003; Bellomo and Delitala, 2008 and the references therein). These models are described in terms of an "activity" variable that characterizes the discrete biological states of individual cells (for example, the degree of recognition of cancer cells by the antigen-presenting cells (Kolev, 2003), or the degree of activation of immune cells, Brazzoli et al., 2010). The need to average over the "activity space" renders these models quite complex (they are described by integro-differential equations), and their complexity is further increased when a spatial component is added (see, for example, the review of Bellomo and Delitala, 2008).

In this article, our focus is on a different class of models, namely non-spatial models described by ordinary differential equations (ODE) (see, for example, Adam and Bellomo, 1997; Dullens et al., 1986; Bajzer et al., 1996; Sachs et al., 2001; Nagy, 2005; Eftimie et al., 2010). These ODE models are based on the assumption that cell populations are homogeneous (each cell has the same "activity" state, which is the average of the activity states of the entire cell population). While these models do not address spatial spread, they provide a much simpler framework within which to explore the interactions among tumor cells and the different types of immune and healthy tissue cells. Such ODE models have been used, for example, to investigate the anti-tumor role of NK cells, $CD8^+$ T cells, $CD4^+$ T cells, B cells (Kuznetsov et al., 1994; Szymanska, 2003; de Pillis et al., 2006; Joshi et al., 2009), and macrophages (Owen and Sherratt, 1998).

We recently reviewed ODE models from a structural point of view (Eftimie et al., 2010), and showed that building these models in steps can help clarify underlying immuno-oncological mechanisms. For the present paper, we took a similar approach and investigated the interactions between Th1 and Th2 cells and tumor cells by increasing model complexity in steps. We derived two parallel mathematical models to investigate separately the Th1-tumor interactions and the Th2-tumor interactions. First, we investigated a model where the Th1 and Th2 cells suppress tumor growth through cytokine production. In this case, there was no direct interaction between the tumor cells and the immune cells. This model contrasts previous mathematical modeling efforts, which have focused on cytotoxic cells that eliminate tumors through direct interactions (see for example Kirschner and Panetta, 1998). Then, we increased model complexity in order to investigate the influence of granulocyte (i.e., eosinophil and neutrophil) recruitment into the tumor microenvironment: Th1 cells preferentially recruit neutrophils while Th2 cells promote eosinophil recruitment (Buonocore et al., 2004; Mattes et al., 2003; Tepper et al., 1992).

Our analysis of the models revealed that in the absence of eosinophils and neutrophils, neither the Th1 nor the Th2 models eliminate the tumor. The recruitment of neutrophils did not have a substantial effect on the dynamics of the Th1 cells. By contrast, the recruitment of eosinophils changed the dynamics of the system substantially, through effects on particular parameters (i.e., the rate of tumor growth, the rate at which Th cells are inactivated after interactions with the tumor cells, the decay rate of tumor-promoting cytokines, the decay rate of type 2 cytokines, and the rate at which the tumors produce cytokines and other factors that support their growth), ultimately leading to elimination of the tumor cells. Moreover, we found that tumor persistence is associated with a critical threshold of the ratio of cytokines that inhibit tumor growth to those that promote tumor growth. Since these results depend on the values of the parameters, we conducted a sensitivity analysis that indicates which parameters are most likely to induce tumor regression. Our modelling reveals a previously unappreciated feedback mechanism between Th2 cells and eosinophils that sustains anti-tumor immunity and promotes tumor rejection.

2. Model description

Many of the immunological processes that will concern us (e.g., recruitment of immune cells into the tumor, tumor growth, and tumor cell lysis by the immune cells and cytokines) are fundamentally spatial processes. However, since we have no explicitly spatial data, we focus on non-spatial models. Following the approach in Yates et al. (2000), we assume that the rates of change of antigen-specific Th1 and Th2 cell populations can be described by

$$\text{Rate} = \text{activation} + \text{proliferation/recruitment} - \text{death}. \quad (1)$$

Throughout this paper we investigate only the dynamics that take place inside the tumor microenvironment. The proliferation/recruitment term describes the fact that the immune cells can either proliferate inside the microenvironment, or proliferate somewhere else and then be recruited into the microenvironment with the help of cytokines and chemokines. For simplicity, we combine the proliferation and recruitment of cells into a single term. The activation term incorporates the rate of successful encounters of naïve cells with antigen presenting cells. Variation in the concentration of antigens can thus alter the activation rate. The time-evolution of tumor cells can be described by a similar equation which has only the growth and the death terms (i.e., no activation for the tumor cells).

In a similar manner, we can describe the rate of change of cytokine concentration via

$$\text{Rate} = \text{production} - \text{decay}. \quad (2)$$

To understand the mechanisms that can lead to the elimination of a tumor by Th2 cells and the failure of Th1 cells, we started by investigating only the interactions between these immune cells and the tumor. These interactions are mediated by cytokines produced by the Th1 cells (type 1 cytokines) and the Th2 cells (type 2 cytokines). Since these cytokines can have both pro-tumor and anti-tumor roles, we distinguished between tumor-suppressing cytokines (such as IFN-γ, TNF-α, or IL-4), and tumor-promoting cytokines (such as IL-10). To simplify the models, we also included in the last category some growth factors that have a pro-tumor effect (such as TGF-β and VEGF).

Our models of tumor–immune interactions use the following notation:

X_{Th}	Th cell population. Under the influence of the cytokine medium, the Th cells can polarize and become Th1 cells (X_{Th1}) or Th2 cells (X_{Th2})
X_{tum}	Tumor cell population
C_1	Type 1 cytokines (i.e., cytokines secreted by Th1 cells, such as IL-2, IFN-γ).
C_2	Type 2 cytokines (i.e., cytokines secreted by Th2 cells, such as IL-4, IL-5, IL-13);

C_{ts} Tumor-suppressing cytokines (i.e., cytokines produced by various immune cells to suppress tumor growth: e.g., IL-4 produced by Th2 cells, tumor necrosis factor α (TNF-α) and interferon γ (IFN-γ) produced by Th1 cells);

C_{tp} Tumor-promoting cytokines (i.e., cytokines produced by tumors and in some cases by immune cells, which promote tumor growth and angiogenesis: VEGF, TGF-β, and even IL-10 and IL-13).

Eqs. (1) and (2) illustrate the terms that will appear in our formal mathematical equations describing the time-evolution of cell populations and cytokine concentrations. Before presenting these equations, we discuss in detail the terms describing the dynamics of each type of cell and class of cytokines.

1. Terms in Eq. (1) associated with Th cells:
   - Activation happens in the presence of tumor cells and is determined by type 2 cytokines (for the Th2 cells) or type 1 cytokines (for the Th1 cells). Moreover, Th cell activation is inhibited by tumor promoting cytokines (TGF-β) (Yates et al., 2000). This interaction can be described mathematically by the term $(a_{Th}C_i/(1+k_pC_{tp}))X_{tum}/(h_2+X_{tum})$, where a_{Th} is the activation rate, C_i stands for type i cytokines ($i=1$ or 2) and k_p determines the concentration of tumor-promoting cytokines at which their effect becomes important. The factor $X_{tum}/(h_2+X_{tum})$ mimics the saturation of interactions between tumor cells and antigen presenting cells as the tumor increases in size. Here h_2 is the half-saturation constant for the tumor cells that are detected by the T cells (via antigen presenting cells).
   - Proliferation happens in the tissue once the cells become activated, and is inhibited by pro-tumor cytokines (TGF-β). Throughout this article we assume that there is a carrying capacity ($1/K_{Th}$) for the total number of Th cells present in the tumor microenvironment. Denoting the proliferation rate by b_{Th}, we can model this proliferating process using $b_{Th}X_{Th}/((1-K_{Th}X_{Th})(1+k_pC_{tp}))$.
   - Cells undergo apoptosis at a constant rate c_{Th}. Moreover, Th cells can become inactivated at a rate d_{Th} after interactions with the tumor cells (Flynn and Stockinger, 2003). We model these two processes via $c_{Th}\,f_{death}\,(X_{Th})+d_{Th}X_{Th}\,X_{tum}$. The apoptosis function f_{death} is slightly different for the Th1 and the Th2 cells. In particular, it has been suggested that a high concentration of IL-2 decreases the death rate of $CD4^+$ T cells (Ganusov et al., 2007). Since IL-2 is a type 1 cytokine, we will assume that it influences the death rate of the Th1 cells, and not the Th2 cells. This might not be entirely realistic, but it helps us to keep the models simple, without introducing another category of cytokines for the Th2 model. We incorporate the effect of IL-2 into the Th1 model by assuming that

$$f_{death}(X_{Th}) = \frac{X_{Th}}{1+k_1C_1}. \tag{3}$$

   For the Th2 model, the apoptosis function is

$$f_{death}(X_{Th}) = X_{Th}. \tag{4}$$

2. Terms in Eq. (1) associated with the dynamics of tumor cells:
   - Tumor growth is modeled by a logistic term that accounts for the deceleration in the growth as the size of the tumor increases (Spratt et al., 1993): $a_{tum}\,X_{tum}\,(1-K_{tum}\,X_{tum})$. Here a_{tum} is the growth rate, and $1/K_{tum}$ is the carrying capacity. Moreover, both the tumor-promoting and tumor-suppressing cytokines affect tumor growth by increasing or decreasing it, respectively. Hence, the full term describing the growth of the tumor is: $a_{tum}X_{tum}(1-K_{tum}X_{tum})(1+k_pC_{tp})/(1+\ k_sC_{ts})$. Here k_p and k_s determine the concentration of tumor-promoting and tumor-suppressing cytokines at which their effects become important.
   - Tumor cells are killed through interactions with tumor-supressing cytokines (Hung et al., 1998): $g_{tum}C_{ts}X_{tum}/(h_0+X_{tum})$. Here g_{tum} is the rate at which the tumor cells are killed by the cytokines, and h_0 is the half-saturation constant for the tumor cells killed by these cytokines.
3. Terms in Eq. (2) associated with the dynamics of type 1 and type 2 cytokines:
   - Production of cytokines is driven by the presence of tumor cells ($X_{tum}/(h_2+X_{tum})$), and is inhibited by the presence of tumor promoting cyokines (TGF-β). Type 1 cytokines are produced by Th1 cells ($i_{11}X_{Th1}$), while type 2 cytokines are produced by Th2 cells ($i_{11}X_{Th2}$). Moreover, the cytokines may be produced at a rate c by other types of cells present in the tumor microenvironment. Putting these effects together, the rate of change of the cytokine population is $(i_{11}X_{Th}+c)X_{tum}/((h_2+X_{tum})(1+k_pC_{tp}))$.
   - Cytokines decay at a constant rate j_0, yielding terms j_0C_i, $i\in\{1,2\}$.
4. Terms in Eq. (2) associated with the dynamics of tumor-suppressing cytokines (e.g., TNF-α, IFN-γ, IL-4):
   - Production of cytokines is driven by the presence of tumor cells, and inhibited by the presence of tumor-promoting cyokines. The cytokines are secreted by Th1 and Th2 cells ($i_{21}X_{Th}$), and possibly by other types of immune cells present in the microenvironment (c). The full term describing the production of these cytokines is $(i_{21}X_{Th}+c)X_{tum}/((h_2+X_{tum})(1+k_pC_{tp}))$.
   - The cytokines decay at a constant rate j_{ts}, yielding the term $j_{ts}C_{ts}$.
5. Terms in Eq. (2) associated with the dynamics of tumor-promoting cytokines (e.g., TGF-β, VEGF, IL-13):
   - Following the approach of Arciero et al. (2004), we model the production of tumor-promoting cytokines by the tumor cells with the term $i_{3t}X_{tum}^2/(h_1^2+X_{tum}^2)$. However, the Th2 cells—and in a smaller proportion the Th1 cells—can produce IL-13, which has pro-tumor effect, being associated with increased tumor implantation (see Mattes et al., 2003). In addition, we account for the production of tumor-promoting cytokines (at rate c) by other cells in the tumor microenvironment (e.g., tumor-associated macrophages). Note that these tumor-promoting cytokines do not seem to be inhibited by any other types of cytokines (such as tumor-supressing cytokines). Putting these various contributions together, the rate of growth of the population of tumor-promoting cytokines is $(i_{31}X_{Th}+c)X_{tum}/(h_2+X_{tum})+i_{3t}X_{tum}^2/((h_1^2+X_{tum}^2))$.
   - The tumor-promoting cytokines decay at a constant rate j_{tp}, yielding the term $j_{tp}C_{tp}$.

Substituting all the above terms into Eqs. (1) and (2), we obtain the following model, which describes the interactions between the Th1 cells and the tumor (the Th1 *model*) or between the Th2 cells and the tumor (the Th2 *model*):

$$\frac{dX_{Th}}{dt} = a_{Th}C_i\frac{X_{tum}}{(h_2+X_{tum})(1+k_pC_{tp})} + \frac{b_{Th}}{1+k_pC_{tp}}X_{Th}(1-K_{Th}X_{Th}) - c_{Th}f_{death}(X_{Th}) - d_{Th}X_{Th}X_{tum}, \tag{5a}$$

$$\frac{dX_{tum}}{dt} = a_{tum}\frac{(1+k_pC_{tp})}{(1+k_sC_{ts})}X_{tum}(1-K_{tum}X_{tum}) - \frac{g_{tum}C_{ts}X_{tum}}{(h_0+X_{tum})}, \tag{5b}$$

$$\frac{dC_i}{dt} = -j_0 C_i + \frac{(i_{11}X_{\rm Th}+c)X_{\rm tum}}{(h_2+X_{\rm tum})(1+k_{\rm p}C_{\rm tp})}, \tag{5c}$$

$$\frac{dC_{\rm ts}}{dt} = -j_{\rm ts}C_{\rm ts} + \frac{(i_{21}X_{\rm Th}+c)X_{\rm tum}}{(h_2+X_{\rm tum})(1+k_{\rm p}C_{\rm tp})}, \tag{5d}$$

$$\frac{dC_{\rm tp}}{dt} = -j_{\rm tp}C_{\rm tp} + \frac{(i_{31}X_{\rm Th}+c)X_{\rm tum}}{(h_2+X_{\rm tum})} + \frac{i_{3t}X_{\rm tum}^2}{(h_1^2+X_{\rm tum}^2)}. \tag{5e}$$

Here, C_i denotes the type i cytokines ($i \in \{1,2\}$) produced by the Th1 or Th2 cells. The apoptosis function $f_{\rm death}$ is given by Eqs. (3) and (4). The Th1 and Th2 *models* differ structurally in that they use different functional forms for $f_{\rm death}$; in addition, they differ in the values of parameters that characterize the production of cytokines (see Table 2 in Appendix A).

It would be possible to reduce the number of parameters in our model—as for most models—by non-dimensionalizing. In this paper, because we use some of the model parameters to interpret biological experiments, we prefer to work with a dimensional model. A more specific way to simplify models like ours is to assume that the cytokines evolve on a much faster time scale, and therefore that their dynamics can be described by a steady-state equation (Yates et al., 2000). Separating timescales in this way would eliminate the last three equations in (5), but would replace each occurrence of a cytokine variable in the remaining equations with a very complex expression in $X_{\rm tum}$ and $X_{\rm Th}$. The resulting system is too unwieldy to be amenable to a useful analytical treatment, so there is little to be gained by this approximation. We therefore proceed with analysis of the full five-equation model (5), without making any approximations. Some useful information can be obtained analytically, but most of our analysis is numerical.

3. Steady states and their stability

In preparation for the numerical investigation of the tumor–immune dynamics, we studied analytically the long-time behavior of model (5). In particular, we were interested in the size of different cell populations and cytokine concentrations when the system is at equilibrium.

First, it is easily shown that if the initial data are non-negative (i.e., $C_i(0) \geq 0$, $i \in 1,2$, and $X_i(0) \geq 0$, $i \in \{\rm Th, tum\}$), then the solution is also non-negative (see Appendix B); in particular, any steady state that is reached will be non-negative. Thus the model is biologically well-posed.

Linear analysis reveals the possibility of having two tumor-free steady states and a coexistence steady state. The first tumor-free steady state is characterized by the absence of any tumor cells, immune cells or cytokines:

$$(X_{\rm Th}, X_{\rm tum}, C_i, C_{\rm ts}, C_{\rm tp}) = (0,0,0,0,0), \quad i \in \{1,2\}. \tag{6}$$

This state corresponds to the successful elimination of the tumor.

The second tumor-free steady state is characterized by the absence of tumor cells and cytokines, but the presence of immune cells:

$$(X_{\rm Th}, X_{\rm tum}, C_i, C_{\rm ts}, C_{\rm tp}) = (X^*,0,0,0,0), \tag{7}$$

where $X^* = (b_{\rm Th}-c_{\rm Th})/K_{\rm Th}b_{\rm Th}$, and $i \in \{1,2\}$. Note that this steady state would not arise without the assumption that the recruitment/proliferation of Th cells occurs at a constant rate, as soon as the cells become activated. Moreover, this steady state exists only when the recruitment rate is larger than the apoptosis rate ($b_{\rm Th} > c_{\rm Th}$). Throughout this paper we will ignore this steady state and choose $b_{\rm Th}$ and $c_{\rm Th}$ such that $b_{\rm Th} < c_{\rm Th}$.

Further investigation of the stability of the tumor-free steady states reveals that these states are always unstable. The eigenvalues of the Jacobian matrix associated with (5) are exactly the terms on the main diagonal of this matrix. For Eq. (5b), the value on the main diagonal is the tumor growth rate ($a_{\rm tum}$), which is always positive. All other terms are zero when calculated at the steady states. The only non-zero population at the steady state (the Th cells) does not enter the equation for the tumor growth. Therefore, when the immune cells do not interact directly with the tumor cells, tumor can only be temporarily eliminated. A slight perturbation in the system will cause tumor relapse.

The relapse of the tumor is characterized by the evolution of system (5) towards a coexistence steady state. This state is described by persistent tumor cells, continuous production of cytokines and a small number of activated immune cells:

$$(X_{\rm Th}, X_{\rm tum}, C_i, C_{\rm ts}, C_{\rm tp}) = (X^*_{\rm Th}, X^*_{\rm tum}, C^*_i, C^*_{\rm ts}, C^*_{\rm tp}), \tag{8}$$

with $i \in \{1,2\}$. It is impossible to write down closed-form equations that completely specify this steady state. However, using the equation for the dynamics of tumor cells ($X_{\rm tum}$) one can obtain an expression for $X^*_{\rm tum}$, which depends on the concentrations of tumor-suppressing cytokines and tumor-promoting cytokines:

$$X^*_{\rm tum} = \frac{-(h_0K_{\rm tum}-1)}{2K_{\rm tum}} \pm \frac{\sqrt{(h_0K_{\rm tum}-1)^2 - 4K_{\rm tum}\left(\frac{g_{\rm tum}}{a_{\rm tum}}S^* - h_0\right)}}{2K_{\rm tum}}, \tag{9}$$

where

$$S^* = \frac{C^*_{\rm ts}(1+k_{\rm s}C^*_{\rm ts})}{(1+k_{\rm p}C^*_{\rm tp})}. \tag{10}$$

The number of coexistence steady states depends on the values of the parameters (see Table 1). When S^* is very large (i.e., the concentration of tumor-supressing cytokines is much higher than the concentration of tumor-promoting cytokines), then the tumor is eliminated and there are no coexistence steady states. When S^* is small ($S^* < h_0a_{\rm tum}/g_{\rm tum}$) (i.e., the concentration of tumor-promoting cytokines is higher than the concentration of tumor-supressing cytokines), there is only one coexistence steady state ($X^{*1}_{\rm tum}$). This state is characterized by a very large number of tumor cells. For intermediate values of S^* (i.e., $S^* > h_0a_{\rm tum}/g_{\rm tum}$), the system can evolve towards one of two possible relatively small steady states $X^{*2}_{\rm tum}$ or $X^{*3}_{\rm tum}$, where $X^{*3}_{\rm tum} < X^{*2}_{\rm tum} (< X^{*1}_{\rm tum})$. Hence, the threshold value $S^* = h_0a_{\rm tum}/g_{\rm tum}$ determines whether the system will evolve towards a very large tumor or a small tumor (of two possible sizes). We will come back to this threshold in the following sections, in the context of our numerical simulations.

Table 1
The number of possible coexistence steady states depends on the values of model parameters, as well as the concentration of tumor-suppressing and tumor-promoting cytokines.

	$S^* \leq \frac{a_{\rm tum}}{g_{\rm tum}b_{\rm tum}}\left(\frac{(b_{\rm tum}h_0-1)^2}{4}+h_0\right)$	$S^* \geq \frac{a_{\rm tum}}{g_{\rm tum}b_{\rm tum}}\left(\frac{(b_{\rm tum}h_0-1)^2}{4}+h_0\right)$
$S^* < \frac{h_0a_{\rm tum}}{g_{\rm tum}}$	1 coexistence steady state ($X^{*1}_{\rm tum}$)	no coexistence steady state
$S^* > \frac{h_0a_{\rm tum}}{g_{\rm tum}}$	2 coexistence steady states ($X^{*2}_{\rm tum}$, $X^{*3}_{\rm tum}$)	no coexistence steady state

We denote by $S^* = C^*_{\rm ts}((1+k_{\rm s}C^*_{\rm ts})/(1+k_{\rm p}C^*_{\rm tp}))$. For large S^* (i.e., the concentration of tumor-suppressing cytokines is much larger than the concentration of tumor-promoting cytokines), there are no coexistence steady states. For small S^* (i.e., a higher concentration of tumor-promoting cytokines), there is a coexistence steady state. However, for intermediate values of S^*, it is possible to have two different coexistence steady states.

4. Numerical results

In this section, we summarize our numerical simulations that investigate the growth of tumor cells and how this is affected by the immune cells. The parameters used for these simulations are specified in Table 2, in Appendix A. Note that throughout this paper we focus on a particular parameter space and assume that the majority of parameters have similar values for both the Th1 and the Th2 *models*. The few exceptions are highlighted in bold in Table 2.

Since we want to understand the mechanisms behind the rejection of tumors by Th2 cells and the failure of Th1 cells to reject them, we use initial conditions similar to the ones described in Mattes et al. (2003). In particular, we model the effect of injecting 10^5 tumor cells on day zero. We also assume that at this initial time, there are no activated immune cells or cytokines present at the injection site: $X_{\mathrm{Th1}}=0$, $X_{\mathrm{Th2}}=0$, $C_i=0$, $C_{\mathrm{ts}}=0$, and $C_{\mathrm{tp}}=0$.

Fig. 1 shows the growth of the tumor following the injection of tumor cells. Because these cells are only weakly immunogenic, the immune response is not significant. Moreover, the differences between the two models we mentioned in Section 2 are not sufficient to induce a difference in tumor growth. For both models, the tumor reaches its carrying capacity approximately 20 days after it is introduced.

Next, following the approach in Mattes et al. (2003), we investigate the result of adoptively transferring 10^7 Th1 and Th2 cells into the tumor-bearing mice. The cells are transfered 7 days after the tumor is inoculated. The adoptive transfer can be incorporated into the model by adding a step function (s_0) to Eqs. (5a) which describe the time-evolution of immune cells. This function is different from zero only on the day the treatment is administered:

$$s_0 = \begin{cases} 10^7/\mathrm{day} & \text{if } t \in [7,8], \\ 0 & \text{otherwise.} \end{cases} \tag{11}$$

Fig. 2 shows the effect of adoptive transfer on the dynamics of the Th1 and Th2 *models*. The graphs in panels (a) and (c) show that neither model is capable of eliminating the tumor. The tumor-suppressing cytokines can only temporarily stop the growth of the tumor. The tumor starts growing again 15–20 days after it was introduced (i.e., 1–2 weeks after the adoptive transfer of T cells). Panels (b) and (d) show the ratio

$$S(t) = \frac{C_{\mathrm{ts}}(t)(1+k_s C_{\mathrm{ts}}(t))}{1+k_p C_{\mathrm{tp}}(t)}, \tag{12}$$

of tumor-suppressing cytokines and tumor-promoting cytokines. The dotted horizontal lines show the threshold value $S^*=h_0 a_{\mathrm{tum}}/g_{\mathrm{tum}}$, which determines when the tumor evolves to a larger steady state close to the carrying capacity (see Section 3). These dotted lines seem to be associated with faster tumor growth. Note that tumor grows fast when $S(t)$ is less than the analytical threshold value S^*. In contrast, the tumor is controlled by the immune system when $S(t)$ is larger than this value.

For the Th1 *model* (panels (a) and (b)), the adoptive transfer of immune cells on day 7 immediately increases the ratio $S(t)$ above the threshold S^*. This leads to a decrease in the tumor size by approximately 5%. For the Th2 *model* (panels (c) and (d)), the increase in $S(t)$ is much smaller. This causes a smaller decrease (of about 0.1%) in tumor size, followed by faster growth.

We also tested the effects of a second adoptive transfer 7 days after the first transfer (as in Mattes et al., 2003), but found only a delay in tumor growth, and no significant tumor cell death. Further investigation of the effects of these adoptive transfers suggested that the tumor can eventually be eliminated if the injections are administered repeatedly until the tumor size is below 2×10^6 cells (not shown here). At this point, one final transfer of immune cells is enough to kill all remaining tumor cells. The number of injections that must be administered depends on the rate of tumor-killing by cytokines (g_{tum}). For example, if $g_{\mathrm{tum}}=3$ (cells/day)(pg/ml)$^{-1}$, then six injections administered within 10 days of each other can eliminate the tumor in approximately 70 days. However, if $g_{\mathrm{tum}}=2$ (cells/day)(pg/ml)$^{-1}$ then eight injections are necessary to eliminate the same tumor. These results describe the outcome of the Th1 *model*. For the Th2 *model* the results are quite similar, the only difference being that tumor elimination is slower and requires longer treatment.

Overall, model (5) cannot explain the experimental results in Mattes et al. (2003). Even if we change the parameter values within some relevant parameter ranges (as will be done in Section 6), we do not observe a situation where the tumor is eliminated in the presence of Th2 cells but not in the presence of Th1 cells.

5. Extension of the Th1 and Th2 models

The models investigated in Sections 3 and 4 considered an anti-tumor effect which was mediated by the release of tumor-suppressing cytokines from CD4$^+$ T cells. However, both the Th1 and Th2 cells have the capacity to recruit other immune cells such as granulocytes (e.g., neutrophils and eosinophils) to the site of inflammation. Granulocytes are short-lived effector cells that can mediate tumor rejection through the release of toxic granules. Mattes et al. (2003) showed that eotaxin, the chemokine involved

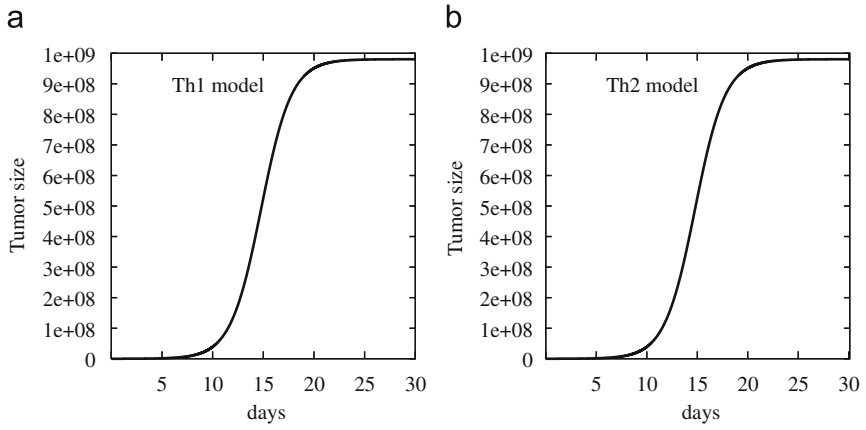

Fig. 1. The dynamics of the Th1 and Th2 *models*. (a) tumor size for the Th1 model; (b) tumor size for the Th2 model. Here $a_{\mathrm{Th}}=0.008$. The rest of the parameters are specified in Table 2, in Appendix A.

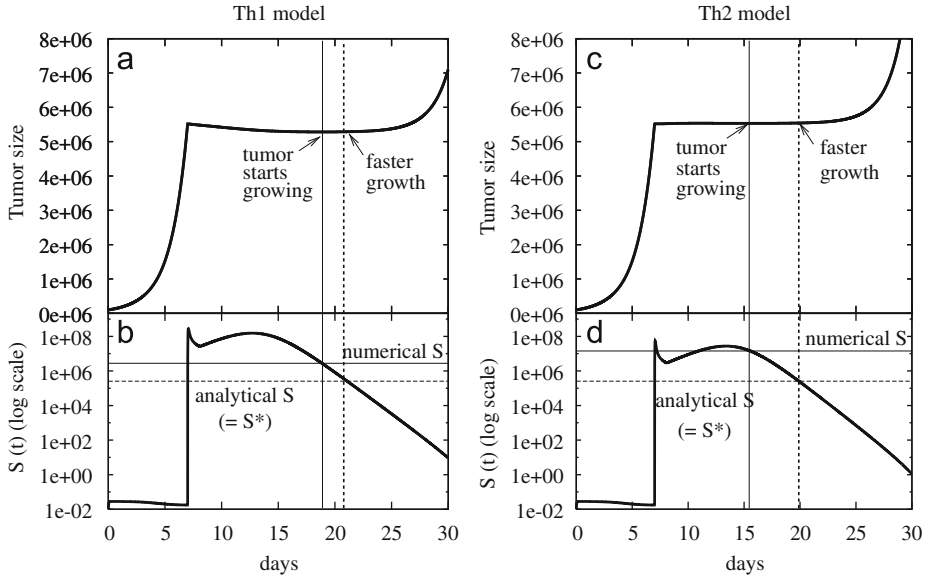

Fig. 2. The dynamics of the Th1 and the Th2 *models*, when 10^7 Th cells are adoptively transfered into the system. (a) Tumor size for the Th1 *model*; (b) Ratio $S(t)=(1+k_sC_{ts}(t))C_{ts}(t)/(1+k_pC_{tp}(t))$ of tumor-suppressing cytokines (C_{ts}) and tumor-promoting cytokines (C_{tp}) for the Th1 *model*. The two horizontal lines show the critical threshold values for S that lead to tumor growth: the numerical S line is calculated by substituting the numerical values for C_{ts} and C_{tp} (at the time when the tumor starts growing again) into the formula for $S(t)$; the analytical S line is $S^*=h_0a_{tum}/g_{tum}$ (i.e., the threshold value which determines when the tumor evolves to a larger steady state (see Section 3)). This analytical line seems to be associated with a faster tumor growth; The continuous vertical line shows the exact time when the tumor is first observed (numerically) to grow, while the dotted vertical line shows the time when the ratio $S(t)$ crosses the analytical threshold $S=S^*$. (c) Tumor size for the Th2 *model*; (d) Ratio $S(t)$ for the Th2 model. Here $a_{Th}=0.008$. The rest of the parameters are specified in Table 2, in Appendix A.

in the recruitment of eosinophils, is correlated with the elimination of tumor by the Th2 cells. Similarly, other studies have shown that neutrophils influence the priming and the polarization of Th1 cells (van Gisbergen et al., 2005), and are involved in anti-tumor immunity (Carlo et al., 2001). In this Section, we extend the Th1 *model* to incorporate neutrophil recruitment, and the Th2 *model* to incorporate eosinophil recruitment.

To describe the dynamics of granulocytes inside the tumor microenvironment, we use again Eq. (1), with details specified as follows:

- Granulocyte activation occurs in the presence of tumor cells. For eosinophils, activation is determined by type 2 cytokines such as IL-5 (Kataoka et al., 2004), while for neutrophils it is determined by tumor-suppressing cytokines such as TNF-α (Carlo et al., 2001). In both cases, cell activation is inhibited by tumor promoting-cytokines. We model these interactions via the term $a_{gran}\hat{C}X_{tum}/(h_2+X_{tum})(1+C_{tp})$, where
$$\hat{C}=\begin{cases} C_2 & \text{for eosinophils} \\ C_{ts} & \text{for neutrophils.} \end{cases} \tag{13}$$
- Eosinophil recruitment is caused by type 2 cytokines (IL-5), while neutrophil recruitment is caused by tumor-suppressing cytokines (TNF-α) (Canetti et al., 2006). In both cases, cell recruitment can be inhibited by tumor-promoting cytokines. In addition, we assume that there is a carrying capacity $(1/K_{gran})$ determining the maximum size of the granulocyte population that can be sustained by the environment. Thus, the full term describing the recruitment of granulocytes is $b_{gran}(1-K_{gran}X_{gran})\hat{C}/(1+k_pC_{tp})$.
- All cells undergo apoptosis at a constant rate c_{gran}: $c_{gran}\,f^g_{death}\,(X_{gran})$. The apoptosis function f^g_{death} is slightly different for the eosinophil and the neutrophil populations. In particular, eosinophil apoptosis is enhanced by tumor suppressing cytokines and reduced by type 2 cytokines (such as IL-5) (Yamagughi et al., 1988):
$$f^g_{death}(X_{gran})=X_{gran}\frac{1+k_pC_{tp}}{1+k_2C_2}. \tag{14}$$
For neutrophils, it has been shown that TNF-α has a dual effect on apoptosis by increasing as well as decreasing it in a concentration-dependent manner (Cross et al., 2007). To simplify the model, we ignore this dual effect and define
$$f^g_{death}(X_{gran})=X_{gran}. \tag{15}$$

Finally, we consider also the twofold anti-tumor effect of granulocytes (that is, direct killing via degranulation or phagocytosis, or indirect killing via tumor-suppressing cytokines) to obtain the following extended model:

$$\frac{dX_{Th}}{dt}=a_{Th}C_i\frac{X_{tum}}{(h_2+X_{tum})(1+k_pC_{tp})}+\frac{b_{Th}}{1+k_pC_{tp}}X_{Th}(1-K_{Th}X_{Th}) -c_{Th}f_{death}(X_{Th})-d_{Th}X_{Th}X_{tum}+s_0, \tag{16a}$$

$$\frac{dX_{gran}}{dt}=a_{gran}\hat{C}\frac{X_{tum}}{(h_2+X_{tum})(1+k_pC_{tp})}+b_{gran}(1-K_{gran}X_{gran})\frac{\hat{C}}{(1+k_pC_{tp})} -c_{gran}f^g_{death}(X_{gran}), \tag{16b}$$

$$\frac{dX_{tum}}{dt}=a_{tum}\frac{(1+k_pC_{tp})}{(1+k_sC_{ts})}X_{tum}(1-K_{tum}X_{tum}) -\frac{g_{tum}C_{ts}X_{tum}}{(h_0+X_{tum})}-\frac{e_{tum}X_{gran}X_{tum}}{(h_0+X_{tum})}, \tag{16c}$$

$$\frac{dC_i}{dt}=-j_0C_i+\frac{(i_{11}X_{Th}+i_{1g}X_{gran}+c)X_{tum}}{(h_2+X_{tum})(1+k_pC_{tp})}, \tag{16d}$$

$$\frac{dC_{ts}}{dt} = -j_{ts}C_{ts} + \frac{(i_{21}X_{Th} + i_{2g}X_{gran} + c)X_{tum}}{(h_2 + X_{tum})(1 + k_p C_{tp})}, \tag{16e}$$

$$\frac{dC_{tp}}{dt} = -j_{tp}C_{tp} + \frac{(i_{31}X_{Th} + c)X_{tum}}{(h_2 + X_{tum})} + \frac{i_{3t}X_{tum}^2}{(h_1^2 + X_{tum}^2)}. \tag{16f}$$

The extended Th1 *model* (i.e., the Th1-*neutrophils model*) and the extended Th2 *model* (i.e., the Th2-*eosinophils model*) differ in their expressions for $f_{death}(X_{Th})$, $\hat{C}$, and f^g_{death} (X_{gran}), as well as their cytokine production rates (see Table 2 in Appendix A). Similar to the models presented in Section 2, these new models evolve towards two tumor-free steady states, or towards some coexistence steady states. As before, the tumor-free states are unstable, because the steady states for both eosinophils and neutrophils are zero ($X^*_{gran}=0$). Thus, the granulocytes are eventually eliminated from the tumor microenvironment and the tumor relapses.

5.1. Numerical results

We studied the dynamics of the two extended models through numerical simulations. The majority of the parameters are similar to those used in Section 4. The new parameters that characterize the dynamics of eosinophils and neutrophils are described in Table 2 in Appendix A.

The dynamics of the extended Th1 and Th2 *systems* are shown in Figs. 3 and 4. As before, we investigated the effect of adoptively transferring 10^7 immune cells on day 7. Comparing Figs. 3 and 4, we observe that adding eosinophils to the Th2 *model* can eliminate the tumor (Fig. 4(a)), while adding neutrophils to the Th1 *model* can only delay the tumor growth (Fig. 3(a)).

For the Th1-*neutrophils model*, even though the curve describing the evolution of the tumor cells (Fig. 3(a)) is qualitatively similar to the one for the model without neutrophils (Fig. 2(a)), they are quantitatively different. We notice that introducing neutrophils reduces the size of the tumor by 14% (from a maximum on day 30 of 7×10^6 cells in Fig. 2(a), to only 6×10^6 cells in Fig. 3(a)). The adoptive transfer of Th1 cells leads to a spike in this cell population (panel (b)). This causes a spike in the concentration of tumor-suppressing cytokines (panel (c)), as well as type 1 cytokines. It also causes a spike in the population of neutrophils recruited at the site (panel (d)). Overall, these immune responses stop tumor growth, and even slightly reduce the size of the tumor. However, the subsequent decrease in the Th1 cell population leads to a decrease in the ratio $S(t)$ (Eq. (12)) and the neutrophil population. Note that for this extended model, the threshold $S^*=h_0a_{tum}/g_{tum}$ is slightly greater than the threshold value that results from the steady-state analysis (which depends also on the steady state for the granulocytes). However, as in Section 4, fast tumor growth is associated with $S(t)$ decaying below S^*.

For the Th2-*eosinophils model*, elimination of the tumor cells results from the combined effects of Th2 cells and eosinophils. In Fig. 4(a) we observe that the decrease in the tumor size starts around day 20. During this time, only the Th2 cells are present in a sufficient number to stop tumor growth (panel (b)). The eosinophils are still being recruited at the site (panel (d)). The decrease in the tumor size is also associated with a ratio $S(t)$ above the critical threshold S^* (panel (c)).

Note that for the Th2 model, the rate at which the tumor is eliminated depends on the parameter values. In particular, significantly increasing the recruitment rate of eosinophils (b_{eos}) or the rate at which these cells kill the tumor (e_{tum}), leads to faster elimination of tumor cells (not shown here). Moreover, even though Fig. 4(a) indicates that there is no tumor after 120 days, careful inspection of the simulation data shows that there are still a few tumor cells left, which will grow again eventually.

We have so far presented results for simulations employing particular parameter values. In the next section we examine the robustness of our results to small changes in parameter values.

6. Sensitivity analysis

There are at least two important reasons to investigate the sensitivity of our results to small changes in parameter values. The first is that none of the parameter values is known precisely and some have had to be guessed (e.g., cytokine production rates), so we need some reassurance that any general conclusions we draw are valid throughout the plausible ranges of each parameter. The second reason is that our ultimate goal is to discover ways to improve immunotherapies for cancer treatment, and to do so we need to know which parameters would be most useful to alter.

In this section, we perform a local sensitivity analysis for the Th1 and Th2 *models*, i.e., we vary one parameter at a time, keeping all other parameters constant. For each parameter, we compare the effects of changes of the same magnitude on the behavior of each of our models. In particular, performing sensitivity analysis on the extended Th1 and Th2 models allows us to investigate how eosinophil and neutrophil recruitment changes the effect that the various model parameters have on tumor growth.

For both models, we start with a parameter set and initial conditions for which tumor is still present after 30 days, and investigate the effect of changing slightly (by 10%) the values of the parameters. (Note that varying the tumor intrinsic growth rate (a_{tum}) by 10% leads (unsurprisingly) to very large changes in tumor size, so we vary a_{tum} only by 1%.) Thus for each parameter, denoting by q the value listed in Table 2, we consider the effect of changing q to $q+\Delta q$, for Δq either positive or negative and $|\Delta q/q| = 0.1$ or 0.01. The result of changing q to $q+\Delta q$ is to change the tumor size after 30 days from X to $X+\Delta X$. In order to compare the effects of changing different parameters, we quantify the change in X as the ratio of relative changes,

$$\frac{\Delta X}{X} \Big/ \left|\frac{\Delta q}{q}\right|. \tag{17}$$

Using this quantity as a metric, Fig. 5 shows how tumor size changes when parameter values are increased or decreased by 1% or 10%. Negative (positive) values correspond to reductions (increases) in tumor size.

Figs. 5(a) and (c) show that in the absence of eosinophils and neutrophils, the parameters that have the most significant impact on tumor size are: tumor growth rate (a_{tum}), the rate at which Th cells are inactivated after interactions with the tumor cells (d_{Th}), the rate at which tumor-promoting cytokines are secreted by the tumor cells (i_{3t}), and the decay rate of tumor promoting cytokines (j_{tp}). A much smaller effect on tumor size is observed when changing the decay rate of tumor suppressing cytokines (j_{ts}) or the apoptosis rate of Th cells (c_{Th}). Note that for all parameters, the direction of the effect is the same for both the Th1 and Th2 *models*.

Figs. 5(b) and (d) show that the dynamics of the extended models depend on the particular types of granulocytes introduced into the system. More precisely, the recruitment of neutrophils by the Th1 cells does not influence the parameters that have a significant effect on the tumor size. However, the recruitment of eosinophils by the Th2 cells greatly decreases the effect of changing d_{Th}. It also decreases the effect of i_{3t}, and increases the effect of the decay rate for type 2 cytokines (j_0). Moreover, the introduction of eosinophils brings in two new parameters that have a significant effect on tumor size (the rate at which

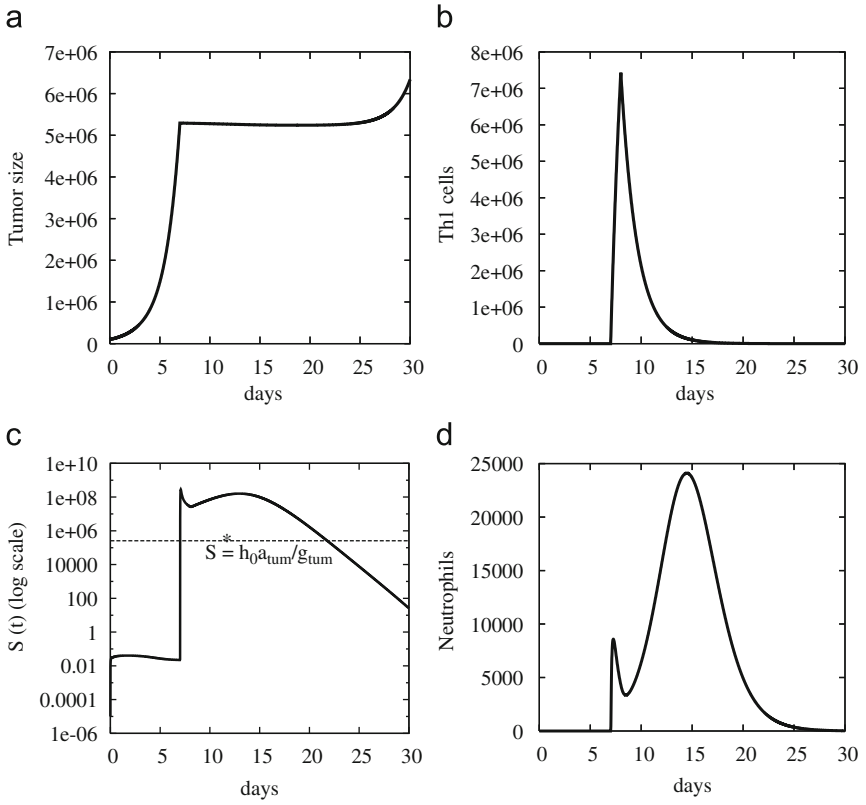

Fig. 3. The dynamics of the Th1 *system* after 10^7 Th1 cells are transfered into the tumor microenvironment on day 7: (a) Tumor cell population; (b) Th1 cell population; (c) Ratio of tumor-suppressing cytokines and tumor-promoting cytokines; The thin horizontal dotted line shows the threshold $S^*=h_0a_{tum}/g_{tum}$ which determines when the tumor starts growing faster towards its carrying capacity; (d) Neutrophil population. Here $a_{Th}=0.008$. The values of the rest of the parameters are specified in Table 2 in Appendix A.

eosinophils are recruited into the tumor microenvironment, b_{gran}, and their apoptosis rate, c_{gran}).

In summary, the parameters that have the most significant effect on tumor size are: tumor growth rate (a_{tum}), the recruitment rate of eosinophils (b_{gran}), the apoptosis rate of eosinophils (c_{gran}), the decay rate of tumor-promoting cytokines (j_{tp}), the decay rate of tumor-suppressing cytokines (j_{ts}), the rate at which cytokines are produced by the tumor cells (i_{3t}), and the decay rate of type 2 cytokines (j_0).

Note that this sensitivity analysis suggests that the rate at which tumor cells are lysed by the eosinophils (e_{tum}) has a more important effect on tumor size compared to the rate at which these cells are lysed by tumor-suppressing cytokines (g_{tum}) (see Fig. 5(d)). For the Th1 model, the roles of e_{tum} and g_{tum} seem to be reversed, i.e., the rate at which tumor cells are killed by the tumor-suppressing cytokines is slightly more important than the rate at which these cells are lysed by the neutrophils. The different results shown in Figs. 5(b) and (d) seem to be caused mainly by the difference in the death rate of granulocytes, f^g_{death} (see Eqs. (15)).

7. Discussion

In this article, we derived mathematical models to investigate anti-tumor immunity mediated by Th1 and Th2 cells. Our interest in this question stems from experimental research in our group (Zhang et al., 2009) and other groups (Hung et al., 1998; Mattes et al., 2003), suggesting that Th2 cells have greater capacity than Th1 cells to promote the rejection of skin cancer. In particular, tumor rejection appears to depend upon the recruitment of eosinophils into the tumor bed. To propose hypotheses that might explain this unexpected anti-tumor effector role of Th2 cells, we employed minimalist models that considered either a 2-cell system ($CD4^+$ T cells and tumor cells) or a 3-cell system ($CD4^+$ T cells, tumor cells, and granulocytes).

Both tumor growth and recruitment of T cells and granulocytes into the tumor are spatial processes. However, for simplicity—and because we currently have no spatially explicit data with which to test our models—we used non-spatial models to describe the tumor–immune interactions. Nevertheless, we were able to incorporate spatial effects implicitly using appropriate nonlinear terms. For example, the lysis of tumor cells by tumor-promoting cytokines and granulocytes is described by Michaelis–Menten terms. These terms can account for the tumor–immune interactions in a solid tumor, where only a fraction of the tumor cells come in contact with the cytokines and granulocytes.

7.1. A critical cytokine ratio threshold

Using numerical techniques, we found that neither the Th1 nor the Th2 cells alone could account for tumor elimination. Furthermore, local sensitivity analysis for the model parameters showed that even if we increase or decrease the parameters by 1% or 10%, the final results are unchanged (Fig. 5). We also varied the parameters by 25% (and even increased them by 100%), and the results were still similar (not shown).

Since the $CD4^+$ T cells interact with the tumor via multiple cytokines, we investigated analytically and numerically the role of these cytokines on the growth of the tumor cells. An empirical investigation of the effect of two types of cytokines on tumor growth was conducted by Hamilton and Bretscher (2008b), who focused on the anti-tumor role of Th1 versus Th2 cells and investigated the ratio IFN-γ/ IL-4 (both of which are tumor-

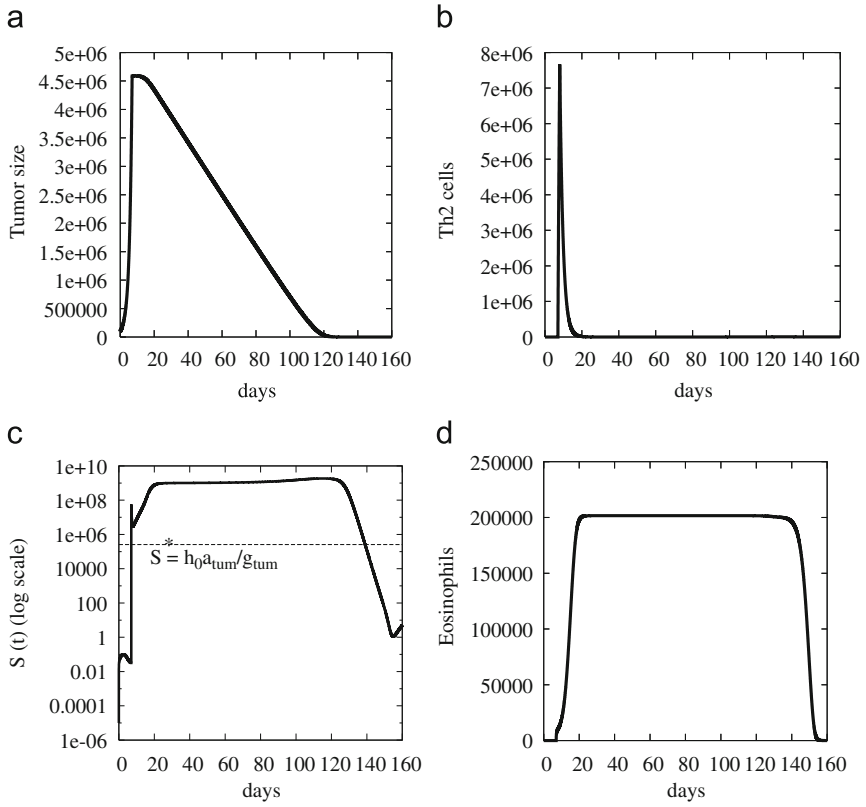

Fig. 4. The dynamics of the Th2 *system* after 10^7 Th2 cells are transferred into the tumor microenvironment on day 7: (a) Tumor cell population; (b) Th2 cell population; (c) Ratio of tumor-suppressing cytokines and tumor-promoting cytokines; The thin horizontal dotted line shows the threshold $S^*=h_0a_{tum}/g_{tum}$ which determines when the tumor starts growing faster towards its carrying capacity; (d) Neutrophil population. Here $a_{Th}=0.008$. The values of the rest of the parameters are specified in Table 2 in Appendix A.

suppresing cytokines). Hamilton and Bretscher (2008b) showed that for two particular tumor lines, regression is associated with a larger ratio. In this paper, we investigated separately Th1 anti-tumor immunity and Th2 anti-tumor immunity. Since there are multiple cytokines that can have an anti-tumor role (including IFN-γ and IL-4), we grouped them together into the class of tumor-suppressing cytokines (C_{ts}). We found that when the ratio of tumor-suppressing to tumor-promoting cytokines ($S(t)$, Eq. (12)) is greater than a certain threshold (S^*), the tumor is controlled by the immune system. In contrast, when $S(t)<S^*$, tumor growth accelerates.

7.2. Tumor control or elimination driven by granulocytes

When granulocytes were added to our models, the simulations began to match the experimental observations (Mattes et al., 2003; Zhang et al., 2009). In particular, the recruitment of neutrophils by the Th1 cells could stop tumor growth and cause some reduction in size. However, the tumors were not rejected. By contrast, the recruitment of eosinophils by the Th2 cells resulted in the elimination of tumor cells. The stronger effect of eosinophils appears to be caused by the large amount of eosinophils recruited into the tumor microenvironment. The eosinophils in turn produced very large concentrations of C_{ts} that contributed to the elimination of the tumor cells.

Note that the temporal delay in the recruitment of eosinophils and neutrophils (see Figs. 3 and 4)—which, in reality, results from a spatial process of migration from the blood to the inflammatory sites in the tissues—was obtained in our model through the explicit incorporation of cytokines. More precisely, the adoptive transfer of T cells leads to an increased production of cytokines, which in turn—after sufficient cytokines have been produced—-triggers the activation and proliferation of granulocytes. Our models do not include any direct interactions between the T cells and the granulocytes.

Our numerical results indicate that the type 2 cytokines produced by eosinophils (e.g., IL-4 Nonaka et al., 1995) strongly promote the elimination of tumor cells by Th2 cells. In particular, when $i_{2g}=0$ tumor growth is temporarily stopped and a large number of tumor cells are killed (not shown here). However, tumor cells start growing again after a few days. When $i_{2g}>0$, the tumor can be eliminated, as shown in Fig. 4(a). By contrast, the production of type 1 cytokines by neutrophils has no impact on tumor growth.

Sensitivity analysis for the models that incorporate granulocytes showed that the results were still valid if we decreased the parameter values by 10% or 25% or increased them by 10%, 25% or 100%. Moreover, this analysis identified parameters that might have a significant effect on the reduction of tumor size (e.g., d_{Th}, i_{3t}, j_{ts} or j_{tp}). Some of these parameters are already the focus of immuno-therapies. For example, experimental studies have shown that injecting the peptide pepstatin into mice leads to an almost 10-fold increase in the serum half-life of IL-2 (a tumor-suppressing cytokine), thus decreasing its decay rate (Ohnishi et al., 1990). However, further experiments should be performed to test whether other parameters are better at decreasing tumor size.

Local sensitivity analysis was also used to get a better understanding of the effect of eosinophils on the size of the tumor cell population. Eosinophils change the dynamics of the tumor–immune system by influencing the way the system responds to changes in particular parameters, such as the decay rate of type 2 cytokines (j_0) or the rate at which the Th cells are inhibited by interactions with the tumor cells (d_{Th}). While increased responsiveness to j_0 was expected (since the eosino-

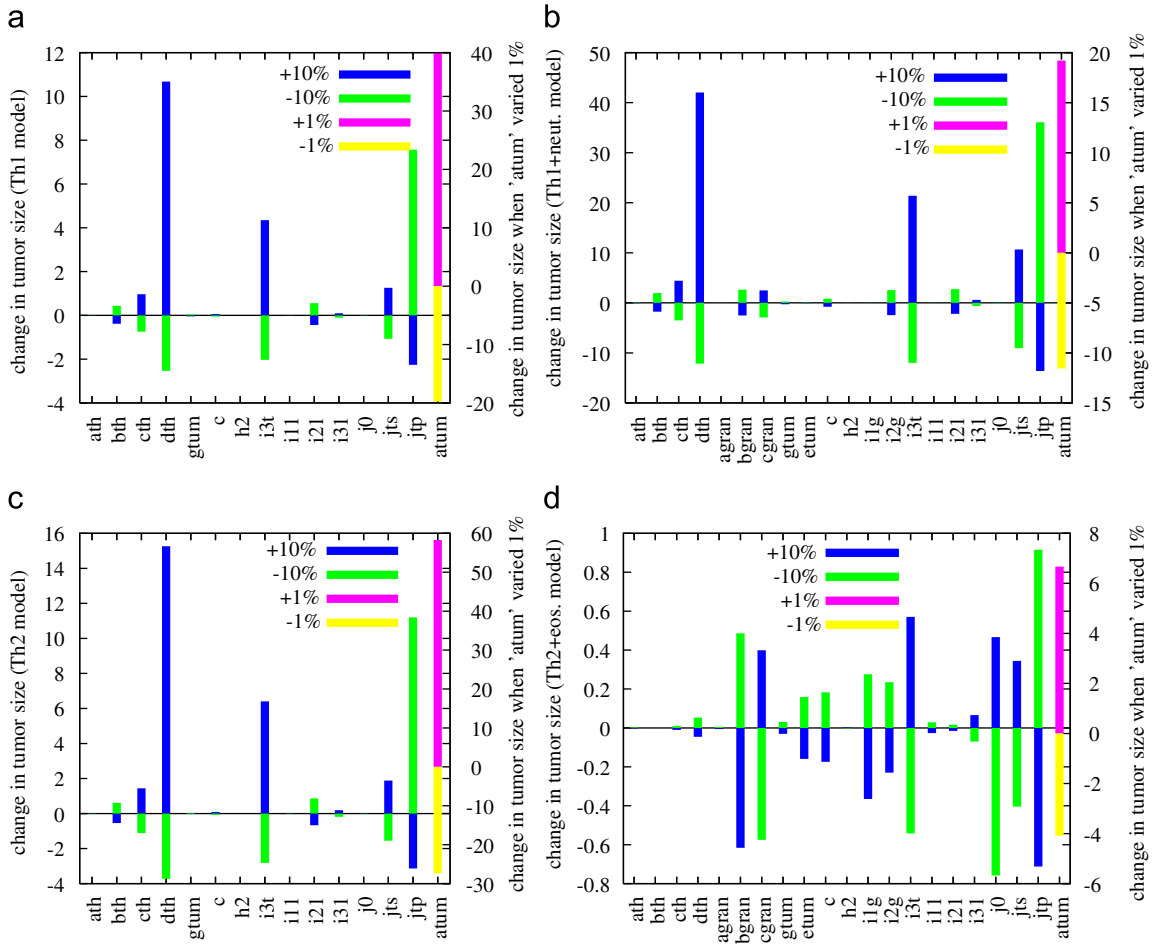

Fig. 5. (Color online) Sensitivity analysis for models (5) and (16). The negative values show the effect of the parameters on decreasing the tumor size, while the positive values show the effect on increasing the tumor size. Also, note that the yellow and magenta rectangles are shown on a secondary axis (on the right-hand-side of the graphs). (a) Th1 *model*; (b) extended Th1 *model* (i.e., the Th1-*neutrophils model*); (c) Th2 *model*; (d) extended Th2 *model* (i.e., the Th2-*eosinophils model*). The dark color (blue and magenta) rectangles show the effect of increasing the parameter values by 10% and 1%. The light color (green and yellow) rectangles show the effect of decreasing the parameter values by 10% and 1%.

phils influence directly the production of type 2 cytokines ($i_{1g} > 0$)), increased responsiveness to d_{Th} was unforeseen, and further work will be required to identify the mechanism behind this behavior.

We also investigated the output of our Th1 and Th2 *models* when various pairs of parameters were altered at the same time. Allowing two parameters to change simultaneously did not yield any surprising results. For example, tumor growth was reduced by decreasing a_{tum} or increasing j_{tp} independently, and was reduced further if both parameter changes were made simultaneously.

7.3. Comparison of model predictions and experiments

A key hypothesis generated by our mathematical models concerns the anti-tumor role of eosinophils versus cytokines. Our sensitivity analysis suggests that the rate of tumor killing by eosinophils through degranulation has a more pronounced effect on tumor size than the rate of tumor killing by tumor-suppressing cytokines. This effect can explain the observation that Th2 cells, which can recruit eosinophils, are more effective at rejecting B16F10 melanoma than Th1 cells, which do not recruit eosinophils.

During the elimination of tumor cells by Th2 cells in our models, we observed that the population of Th cells decreased, while the population of eosinophils increased. Similar dynamics between the lymphocytes and eosinophils have been observed experimentally (Jeong et al., 2007). Whether the mechanisms underlying the experimental results are the same as the ones underlying our mathematical model, remains to be determined.

Another observation is that the tumor-growth curves shown in Figs. 3(a) and 4(a) capture the general dynamics exhibited by various tumor cells. As an example, Hamilton and Bretscher (2008a) investigated experimentally the growth of L5178Y lymphoma cells after the immune system had been previously activated through "excision priming". They found that the growth was suppressed by the Th1 cells, and delayed by the Th2 cells. This contrasts our results for B16F10 melanoma, where the Th2 cells suppress tumor growth (Fig. 4(a)), and the Th1 cells only delay it (Fig. 3(a)). This different outcome is likely the result of distinct tumor–immune dynamics for the two tumor cell lines (L5178Y and B16F10). Nevertheless, it is encouraging that our results capture the general dynamics observed in other cancer cells.

7.4. Conclusions and directions for further research

Our mathematical models have shown that the recruitment of granulocytes (and, in particular, eosinophils) by the $CD4^+$ T cells

impacts tumor growth more significantly than the release of tumoricidal cytokines such as IFN-γ and TNF-α. Consequently, we can now explain the observation that the Th2 cells, which can recruit eosinophils into the tumor microenvironment, are more protective against the B10F16 melanoma than the Th1 cells, which do not recruit eosinophils. However, additional experimental research is required to test our models and further elucidate the mechanisms underlying the interactions between Th cells, tumor cells, and different granulocytes.

Further development of our models will be useful in reconciling the differences between our theoretical results and those of others who—using different tumor models—found that Th1 cells appeared to be more efficient at promoting tumor rejection (Nishimura et al., 1999; Hamilton and Bretscher, 2008a). To identify the source of this difference, our models must be expanded in complexity in order to account for different methods of immunization and the distinct environments of solid tumors and leukemias.

Another potentially fruitful direction for development of our models would be to include a spatial component explicitly. While our non-spatial models already provide an explanation of the observed tumor–immune dynamics, including the spatial component might reveal important mechanisms and lead to a deeper understanding of the tumor–immune interactions (see, for example, the ODE and PDE models proposed by Kuznetsov et al. (1994) and Matzavinos et al. (2004), and by Owen and Sherratt (1998, 1999), to investigate the anti-tumor effect of $CD8^+$ T cells and macrophages). Spatial models would also allow us to investigate the effects of immune cells being recruited into specific regions of a tumor (for example, eosinophils seem to be recruited mostly into the necrotic and capsule region of B16F10 melanoma (Cormier et al., 2006)).

Acknowledgments

This work was supported by Terry Fox New Frontiers Program Project Grant #018005. R.E. thanks A. Llop and M. Colangelo for discussions about granulocytes, and D. Bernard and B. McGray for discussions about tumor–immune dynamics.

Appendix A

Here, we describe the parameter values we use throughout this paper. Some of the values were taken from the published literature (see Table 2 and the references therein). However, this is a first model which investigates the effects of the Th1 cells, Th2 cells, eosinophils and neutrophils on the growth of the tumor. For this reason, not all parameter values could be found in the literature. We will describe in detail how we obtained some of the missing values.

The only parameter values that can be taken from other mathematical models existent in the literature are those describing the dynamics of some particular types of cytokines, the dynamics of tumor cells and $CD4^+$ T cells (although the models do not usually make any distinction between the Th1 and the Th2 cells). For example, the activation rate for the $CD4^+$ T cells in healthy patients is 0.002 (Ribeiro et al., 2002). However, the HIV infected patients have a higher activation rate (between 0.003 and 0.009). Here we will assume that the activation rate for the $CD4^+$ T cells is 0.008.

The values of the parameters that describe the activation, recruitment and death rate of eosinophils and neutrophils are very scarce. Production and decay rates for different types of cytokines are also hard to find. In the following, we will approximate some of these rates using known information about the half-life of cells and cytokines. The relationship between the death (decay) rate and the half-life of cells (cytokines) is given by

$$d=\frac{\ln(2)}{t_{1/2}}, \tag{18}$$

where d represents the death rate, and $t_{1/2}$ represents the half-life time.

Using this formula, we can calculate the values of some of the parameters as follows:

- In the absence of any immune response, Th cells half-life is taken to be approximately 1 week. This translates into a death rate $c_{\mathrm{Th}}=0.1$. We will assume that inside the tumor microenvironment, the level of the Th cells is approximately constant. This means that the recruitment rate balances the death rate, and thus we choose $b_{\mathrm{Th}}=0.09$. We make this assumption to ensure that the immune cells disappear from the microenvironment after the tumor is eliminated (see Eq. (7) and the discussion about it).
- The half-life of eosinophils in the rats blood is approximately 6.7 h (Spry, 1971). Taking an average of 7 h, it results in a decay rate of $c_{\mathrm{eos}}=2.38$. Note that these are blood parameters. It may be possible that the tissue parameters are slightly different. However, since we do not have any information about the rates inside the tumor microenvironment, we will use the blood values. We should also keep in mind that the presence of the tumor will most likely change these rates through the secretion of cytokines.
- For neutrophils, we consider a half-life of 6 hours. This translates into a decay rate $c_{\mathrm{neut}}=2.7$.
- We consider the average half-life of cytokines to be 30 min, which translates into a decay rate $j_i=34$, $i\in\{0,\mathrm{tp},\mathrm{ts}\}$. This half-life value is consistent with the observations for IL-2 (whose half-life seems to be between 30–120 min, Rosenberg and Lotze, 1986), and for TNF-α (whose serum half-life is between 6–20 min, Tracey and Cerami, 1994). The half-life of IL-4 serum levels is also very short, ranging from 15 to 22 min (Alatrash et al., 2005). Note that the majority of the mathematical models that incorporate the effect of different tumor suppressing cytokines consider a half-life of about 90–100 min, which would correspond to $j_i=10$ (see for example Kirschner and Panetta, 1998; Arciero et al., 2004).

To incorporate the production rates of different cytokines into the mathematical models, we have to quantify somehow these rates. To this end, we derive a very simple equation that can approximate the process of cytokine production.

It is known that the cytokines are produced by the cells in an on/off cycling manner (Corbin and Harty, 2005; Slifka et al., 1999). In particular, upon interaction with the antigen, the T cells start producing rapidly cytokines. After the dissociation of T cells from their targets, the production stops immediately. To derive the equation for the production of the cytokines, we focus only on the "on" part of the cycling. Once the tumor is killed the production stops immediately, and this can account for the "off" part of the cycling.

Let us denote by $C(t)$ the concentration of cytokines at time t. Since during the "on" switch the cytokines are produced immediately, we can assume that the concentration of the cytokines follows an exponential dynamics:

$$C(t)=e^{kt}-1 \tag{19}$$

Here, k describes the production rate, while "-1" accounts for the assumption that at $t=0$, the cytokine level is zero. Therefore, the

Table 2
Parameter values for the Th1 and Th2 *models*.

Parameter	Value (Th1 model)	Value (Th2 model)	Units	Description	Reference
a_{Th}	0.008–1.008	0.008–1.008	cell (days^{-1}) (pg/ml)$^{-1}$	Activation rate of Th cells	Ribeiro et al. (2002)
b_{Th}	0.09	0.09	days^{-1}	Proliferation rate of Th cells	guess
c_{Th}	0.1	0.1	days^{-1}	Apoptosis rate of Th cells	guess
K_{Th}	10^{-8}	10^{-8}	cell^{-1}	K_{Th}^{-1}= carrying capacity of Th cells	
k_1	10^{-8}	10^{-8}	(pg/ml)$^{-1}$	k_1^{-1}=concentration of IL-2 (which inhibits the apoptosis of Th1 cells) at half-maximum	Arciero et al. (2004)
k_p	1	1	(pg/ml)$^{-1}$	k_p^{-1}= concentration of C_{tp} at half-maximum (scaled value)	Arciero et al. (2004)
k_s	1	1	(pg/ml)$^{-1}$	k_s^{-1}= concentration of C_{ts} at half-maximum (scaled value)	Arciero et al. (2004)
k_2	1	1	(pg/ml)$^{-1}$	k_2^{-1}= concentration of C_2 at half-maximum (scaled value)	guess
d_{Th}	10^{-7}	10^{-7}	cell^{-1} days^{-1}	Inactivation rate of Th cells by the tumor	de Pillis et al. (2005)
a_{gran}	0.08	0.08	cell (days^{-1}) (pg/ml)$^{-1}$	Activation rate of granulocytes (eosinophils & neutrophils)	guess
b_{gran}	10	10	cell (days^{-1}) (pg/ml)$^{-1}$	Recruitment rate of granulocytes	guess
c_{gran}	**2.38**	**2.7**	days^{-1}	Apoptosis rate of granulocytes	Spry (1971)
K_{gran}	5×10^{-6}	5×10^{-6}	cell^{-1}	K_{gran}^{-1}=carrying capacity of granulocytes	guess
a_{tum}	0.514	0.514	days^{-1}	Tumor growth rate	de Pillis et al. (2005)
K_{tum}	1.02×10^{-9}	1.02×10^{-9}	cell^{-1}	K_{tum}^{-1}=carrying capacity of tumor cells	de Pillis et al. (2005)
g_{tum}	0.2	0.2	(cell)(days^{-1}) (pg/ml^{-1})	Tumor killing rate by the cytokines	Hung et al. (1998)
e_{tum}	**0.2**	**0.085**	days^{-1}	Tumor killing rate by the granulocytes	Mattes et al. (2003) Challacombe et al. (2006)
h_2	10^3	10^3	cell	Half-saturation constant for the tumor cell population detected by the T cells	Arciero et al. (2004)
h_1	10^6	10^6	cell	Half-saturation constant for the Tumor cell population producing tumor-promoting cytokines	Arciero et al. (2004)
h_0	10^5	10^5	cell	Half-saturation constant for the tumor cell population killed by the immune cells and cytokines	Kirschner and Panetta (1998)
j_0	34	34	days^{-1}	Decay rate of type 1 and type 2 cytokines	Rosenberg and Lotze (1986), Tracey and Cerami (1994)
j_{ts}	34	34	days^{-1}	Decay rate of tumor-suppressing cytokines	Rosenberg and Lotze (1986), Tracey and Cerami (1994)
j_{tp}	34	34	days^{-1}	Decay rate of tumor-promoting cytokines	Rosenberg and Lotze (1986), Tracey and Cerami (1994)
i_{11}	**9.0**	**5.4**	(pg/ml) (days^{-1}) cell^{-1}	Production rate of type 1/2 cytokines by the Th cells	Mattes et al. (2003)
i_{1g}	**6.0**	**5.4**	(pg/ml) (days^{-1}) cell^{-1}	Production rate of type 1/2 cytokines by the granulocytes	Mattes et al. (2003)
i_{21}	**6.0**	**8.6**	(pg/ml) (days^{-1}) cell^{-1}	Production rate of tumor-suppressing cytokines by the Th cells	Mattes et al. (2003)
i_{2g}	**8.0**	**3.2**	(pg/ml) (days^{-1}) cell^{-1}	Production rate of tumor-suppressing cytokines by the granulocytes	Mattes et al. (2003)
i_{31}	$\mathbf{2.3\times10^{-4}}$	$\mathbf{3.8\times10^{-4}}$	(pg/ml) (days^{-1}) cell^{-1}	Production rate of tumor-promoting cytokines by the Th cells	guess
i_{3t}	10	10	(pg/ml) (days^{-1})	Production rate of tumor-promoting cytokines by the tumor	guess
c	1	1	pg/ml	Production rate of cytokines by other cells in the microenvironment (cells that are not included specifically in this model)	guess

In bold are those values which are different for the two models.

cytokine production rate is described by

$$\frac{dC}{dt} = kC(t). \tag{20}$$

This says that the production of new cytokines is proportional to the concentration of the existing cytokines. This make sense since some cytokines (e.g., IL-4) are produced in an autocrine manner: the cytokines activate new T cells, which in turn produce even more cytokines. The production rate (k) can be calculated as follows:

$$k = \frac{\ln(C(t)+1)}{t}. \tag{21}$$

Using this simple model, one can approximate the production rates for the different cytokines present in the tumor microenvironment. For this we use data from Mattes et al. (2003). There the authors measured the level of cytokines produced by the Th1 and Th2 cells following a 48 h OVA restimulation. Thus, in Eq. (21) we take the time to be $t=2$ days. The production rates k for various cytokines are approximated as follows:

- For the Th2 cells:
  1. IL-4 production rate: $k_{IL\text{-}4} = \ln(4*10^2+1)/2 = 2.99$.
  2. IL-5 production rate: $k_{IL\text{-}5} = \ln(10^5+1)/2 = 5.756$.
  3. TNF-α production rate: $k_{TNF\text{-}\alpha} = \ln(5*10^2+1)/2 = 3.1$.
  4. IL-13 production rate: $k_{IL\text{-}13} = \ln(2*10^3+1)/2 = 3.8$.
- For the Th1 cells:
  1. IFN-γ production rate: $k_{IFN\text{-}\gamma} = \ln(5*10^4+1)/2 = 5.4$.
  2. TNF-α production rate: $k_{TNF\text{-}\alpha} = \ln(6*10^2+1)/2 = 3.2$.
  3. IL-13 production rates: $k_{IL\text{-}13} = \ln(10^2+1)/2 = 2.3$.

To obtain the rate at which the Th1 and Th2 cells produce tumor-suppressing cytokines, we add the production rates for the different cytokines that belong to this category (see the values in Table 2). We use a similar approach for the type 1 and type 2 cytokines. Note that we use the same values to calculate the rates at which the eosinophils and the neutrophils produce different

types of cytokines (i.e., IL-4 and TNF-α for the eosinophils, and TNF-α for the neutrophils).

The experimental results in Mattes et al. (2003) measured the concentration of the cytokines after 48 h. But it might be possible that these concentrations are already obtained after 24 h. This would imply that the previous rates would be higher. The effect of increasing these rates was investigated in Section 6, and the results did not show any significant differences.

Next, we calculate the rates at which the tumor-suppressing cytokines, the eosinophils and the neutrophils lyse the tumor cells. For this, we use *in vitro* data from the graphs published in Hung et al. (1998) and Mattes et al. (2003) showing the percent lysis as a function of effector:target ratio (E:T). To translate this information into the killing rates that are necessary for the mathematical models, we use a formula derived by Poe et al. (1996). There, the rate for killing at a killer-to-target ratio E:T=r:1 is

$$k_r = \frac{\ln(100)}{\ln(100-\%\text{lysis})}\frac{1}{t}. \tag{22}$$

Here t is the time during which the immune cells are incubated with the tumor cells at a specified E:T ratio. Usually, t=4-6 h. Using this formula and the graphs from Mattes et al. (2003), one can obtain the lysis rate of the tumor cells by the eosinophils at a 1:1 ratio: k_{eos}=0.2. Moreover, using the graphs in Hung et al. (1998), we can find the %lysis by the tumor-suppressing cytokines. Since there is no significant difference between the killing of tumor cells by Th1 or Th2 cytokines, we choose the same killing rate for all the tumor suppressing cytokines: k_{cytok}=0.2. The lysis rate for the neutrophils can be found from Challacombe et al. (2006): k_{neut}=0.085.

We recognize that these rates might not be biologically realistic. Previous results have shown that the *in vivo* rates might be faster than the *in vitro* rates (Regoes et al., 2007). Higher values for these parameters might explain the faster elimination of tumor cells observed experimentally (Mattes et al., 2003). Our numerical results suggested that it takes at least 160 days for the Th2-*eosinophils model* to eliminate the tumor. To counterbalance the low lysis rates we decided to choose large recruitment rates for the granulocytes (i.e., b_{gran}=10). This allows the tumor to be eliminated in approximately 120 days. Note that a faster lysis rate (i.e., e_{tum},$g_{tum} \approx 1$) decreases significantly the time necessary to eliminate the tumor cells (numerical results for this case are not shown in this paper).

Finally, we calculate the carrying capacities for the immune cells. Since 10^6 cells/ml can cause severe eosinophilia, we take the carrying capacity for eosinophils to be $(K_{gran})^{-1} = 1/(5\times 10^{-6})$. We consider a similar value for the carrying capacity of neutrophils. The carrying capacity for the Th cells is $(K_{Th})^{-1}=1/10^{-8}$.

Table 2 summarize the values of the parameters we used for the two mathematical models. Note that some of the rates differ by one or two order of magnitudes (see, for example, the rates of activation, proliferation, and apoptosis of different immune cells). This is the result of experimental data, as well as our guesses for different parameter values which would give patterns that may be biologically realistic.

Appendix B

Here we briefly show that if the initial data is non-negative (i.e., $C_i(0)\geq 0$, $i\in 1,2$, and $X_i(0)\geq 0$, $i\in\{\text{Th,tum}\}$), then the solution is also non-negative. To start, Eqs. (5c)–(5d) are used to show that

$$\frac{dC_i(t)}{dt} \geq -j_i C_i(t), \quad i\in\{1,2\}. \tag{23}$$

This leads to the following inequality

$$C_i(t) \geq C_i(0)e^{-j_i t} \geq 0, \quad \text{for } C_i(0)\geq 0, \quad i\in\{1,2\}. \tag{24}$$

Then, Eq. (5b) is used to show that

$$\frac{dX_{tum}(t)}{dt} > a_{tum}\left(\frac{1+k_pC_{tp}(t)}{1+k_sC_{ts}(t)}\right)X_{tum}(t) - g_{tum}C_{ts}(t)X_{tum}(t). \tag{25}$$

From this, we obtain the following inequality for the size of the population of tumor cells:

$$X_{tum}(t) > X_{tum}(0)e^{\int_0^t (a_{tum}((1+k_pC_{tp}(\tau))/(1+k_sC_{ts}(\tau))) - g_{tum}C_{ts}(\tau))\,d\tau}. \tag{26}$$

Hence, if $X_{tum}(0)\geq 0$ then $X_{tum}(t)\geq 0$, for any $t\geq 0$ for which the solution exists.

Finally, Eq. (5a) is used to show that

$$\frac{dX_{Th}(t)}{dt} \geq \frac{a_{Th}C_i(t)X_{tum(t)}}{(1+k_pC_{tp}(t))(h_2+X_{tum}(t))} + b_{Th}X_{Th}(t), \tag{27}$$

where, $i\in\{1,2\}$. This leads to

$$X_{Th}(t) > X_{Th}(0)e^{b_{Th}t} + \int_0^t \frac{e^{b_{Th}(t-\tau)}a_{Th}C_i(s)X_{tum}(s)}{(1+k_pC_{tp}(s))(h_2+X_{tum}(s))}\,ds. \tag{28}$$

Therefore, if $X_{Th}(0)\geq 0$ then $X_{Th}(t)\geq 0$ for any $t\geq 0$ for which the solution exists.

References

Adam, J., Bellomo, N., 1997. A Survey of Models for Tumor–Immune System Dynamics. Birkhäuser, Boston.

Alatrash, G., Bukowski, R., Tannenbaum, C., Finke, J., 2005. Interleukins. In: Cancer Chemotherapy and Biotherapy Principles and Practice. Lippincott Williams & Wilkins, Philadelphia, pp. 767–809 (Chapter 36).

Algarra, I., Cabrera, T., Garrido, F., 2000. The hla crossroad in tumor immunology. Hum. Immunol. 61 (1), 65–73.

Araujo, R., McElwain, D., 2004. A history of the study of solid tumor growth: the contribution of mathematical modeling. Bull. Math. Biol. 66, 1039–1091.

Arciero, J., Jackson, T., Kirschner, D., 2004. A mathematical model of tumor–immune evasion and siRNA treatment. Discrete Continuous Dyn. Systems Ser. B 4 (1), 39–58.

Bajzer, Z., Maručić, M., Vuk-Pavlović, S., 1996. Conceptual frameworks for mathematical modeling of tumor growth dynamics. Math. Comput. Modelling 23 (6), 31–46.

Behrens, G., Li, M., Smith, C., Belz, G., Carbone, J.M.F., Heath, W., 2004. Helper t cells, dendritic cells and CTL immunity. Immunol. Cell Biol. 82 (1), 84–90.

Bellomo, N., Bellouquid, A., Angelis, E.D., 2003. The modelling of the immune competition by generalized kinetic (Boltzmann) models: review and research perspectives. Math. Comput. Modelling 37, 65–86.

Bellomo, N., Delitala, M., 2008. From the mathematical kinetic, and stochastic game theory to modeling mutations, onset, progression and immune competition of cancer cells. Phys. Life Rev. 5, 183–206.

Bellomo, N., Li, N., Maini, P., 2008. On the foundations of cancer modeling: selected topics, speculations, and perspectives. Math. Models Methods Appl. Sci. 18 (4), 593–646.

Bellomo, N., Preziosi, L., 2000. Modelling and mathematical problems related to tumor evolution and its interactions with the immune system. Math. Comput. Modelling 32, 413–452.

Brazzoli, I., Angelis, E.D., Jabin, P.-E., 2010. A mathematical model of immune competition related to cancer dynamics. Math. Methods Appl. Sci. 33, 733–750.

Buonocore, S., Surquin, M., Moine, A.L., Abramowicz, D., Flamand, V., Goldman, M., 2004. Amplification of T-cell responses by neutrophils: relevance to allograft immunity. Immunol. Lett. 94, 163–166.

Byrne, H., Alarcon, T., Owen, M., Webb, S., Maini, P., 2006. Modeling aspects of cancer dynamics: a review. Philos. Trans. R. Soc. A 364, 1563–1578.

Canetti, C., Silva, J., Ferreira, S., Cunha, F., 2006. Tumor necrosis factor-alpha and leukotriene B_4 mediate the neutrophil migration in immune inflammation. Brit. J. Pharmacol. 364, 1563–1578.

Carlo, E.D., Forni, G., Lolini, P., Colombo, M., Modesti, A., Musiani, P., 2001. The intriguing role of polymorphonuclear neutrophils in antitumor reactions. Blood 97, 339–345.

Challacombe, J., Suhrbier, A., Parsons, P., Jones, B., Hampson, P., Kavanagh, D., Rainger, G.E., Morris, M., Lord, J., Le, T., Hoang-Le, D., Ogbourne, S.M., 2006. Neutrophils are a key component of the antitumor efficacy of topical chemotherapy with Ingenol-3-Angelate. J. Immunol. 177, 8123–8132.

Chaplain, M., 2008. Modelling aspects of cancer growth: insight from mathematical and numerical analysis and computational simulation. Multiscale Problems in the Life Sciences. Lecture Notes in Mathematics, vol. 1940/2008. Springer, Berlin/Heidelberg, pp. 147–200.

Chaplain, M., Kuznetsov, V., James, Z., Stepanova, L., 1998. Spatio-temporal dynamics of the immune system response to cancer. In: Mathematical Models in Medical and Health Sciences. Vanderbilt University Press, Nashville, pp. 1–20.

Corbin, G., Harty, J., 2005. T cells undergo rapid ON/OFF but not ON/OFF/ON cycling of cytokine production in response to antigen. J. Immunol. 174, 718–726.

Cormier, S., Taranova, A., Bedient, C., Nguyen, T., Protheroe, C., Pero, R., Dimina, D., Ochkur, S., O'Neill, K., Colbert, D., Lombari, T., Constant, S., McGarry, M., Lee, J., Lee, N., 2006. Pivotal advance: eosinophil infiltration of solid tumors is an early and persistent inflammatory host response. J. Leukoc. Biol. 79, 1131–1139.

Corthay, A., Skovseth, D., Lundin, K., Rosjo, E., Omholt, H., Hofgaard, P., Haraldsen, G., Bogen, B., 2005. Primary antitumor immune response mediated by $CD4^+$ T cells. Immunity 22 (3), 371–383.

Cross, A., Moots, R., Edwards, S., 2007. The dual effects of TNF-α on neutrophil apoptosis are mediated via differential effects on expression of Mcl-1 and Bfl-1. Blood 111 (2), 878–884.

de Pillis, L., Gu, W., Radunskaya, A., 2006. Mixed immunotherapy and chemotherapy of tumors: modeling, applications and biological interpretation. J. Theor. Biol. 238, 841–862.

de Pillis, L., Radunskaya, A., Wiseman, C., 2005. A validated mathematical model of cell-mediated immune response to tumor growth. Cancer Res. 65 (17), 7950–7958.

Dullens, H., Tol, M.V.D., de Weger, R., Otter, W.D., 1986. A survey of some formal models in tumor immunology. Cancer Immunol. Immunother. 23, 159–164.

Eftimie, R., Bramson, J.L., Earn, D.J.D., 2010. Interactions between the immune system and cancer: a brief review of non-spatial mathematical models. Bull. Math. Biol., doi:10.1007/s11538-010-9526-3.

Flynn, S., Stockinger, B., 2003. Tumor and cd4 t cell interactions: tumor escape as a result of reciprocal inactivation. Blood 101 (11), 4472–4478.

Ganusov, V., Milutinovic, D., de Boer, R., 2007. Il-2 regulates expansion of $cd4^+$ t cell populations by affecting cell death: insights from modeling CFSE data. J. Immunol. 179 (2), 950–957.

Garcia-Lorca, A., Algarra, I., Garrido, F., 2003. Mhc class i antigens, immune surveillance, and tumor immune escape. J. Cell. Physiol. 195 (3), 346–355.

Hamilton, D., Bretscher, P., 2008a. The commonality in the regulation of the immune response to most tumors: the prevalence of immune class deviation as a tumor escape mechanism and its significance for vaccination and immunotherapy. Cancer Therapy 6, 745–754.

Hamilton, D., Bretscher, P., 2008b. Different immune correlates associated with tumor progression and regression: implications for prevention and treatment of cancer. Cancer Immunol. Immunother. 57, 1125–1136.

Hung, K., Hayashi, R., Lafond-Walker, A., Lowenstein, C., Pardoll, D., Levitsky, H., 1998. The central role of $CD4^+$ T cells in the antitumor immune response. J. Exp. Med. 188, 2357–2368.

Jeong, I., Han, K., Joung, J., Choi, W., Hwang, S.-S., Yang, S., Seo, H., Chung, J., Lee, K., 2007. Analysis of changes in the total lymphocyte and eosinophil count during immunotherapy for metastatic renal cell carcinoma: correlation with response and survival. J. Korean Med. Sci. 22 (Suppl.), S122–S128.

Joshi, B., Wang, X., Banerjee, S., Tian, H., Matzavinos, A., Chaplain, M., 2009. On immunotherapies and cancer vaccination protocols: a mathematical modeling approach. J. Theor. Biol. 259 (4), 820–827.

Kataoka, S., Konishi, Y., Nishio, Y., Fujikawa-Adachi, K., Tominaga, A., 2004. Antitumor activity of eosinophils activated by IL-5 and Eotaxin against hepatocellular carcinoma. DNA Cell Biol. 23 (9), 549–560.

Kirschner, D., Panetta, J., 1998. Modeling immunotherapy of the tumor–immune interaction. J. Math. Biol. 37, 235–252.

Kolev, M., 2003. Mathematical modeling of the competition between acquired immunity and cancer. Int. J. Math. Comput. Sci. 13 (3), 289–296.

Kuznetsov, V., Makalkin, I., Taylor, M., Perelson, A., 1994. Nonlinear dynamics of immunogenic tumors: parameter estimation and global bifurcation analysis. Bull. Math. Biol. 2 (56), 295–321.

Lane, C., Leitch, J., Tan, X., Hadjati, J., Bramson, J., Wan, Y., 2004. vaccination-induced autoimmune vitiligo is a consequence of secondary trauma to the skin. Cancer Res. 64 (4), 1509–1514.

Leitch, J., Frazer, K., Lane, C., Putzu, K., Adema, G., Zhang, Q., Jefferies, W., Bramson, J., Wan, Y., 2004. Ctl-dependent and independent antitumor immunity is determined by the tumor not the vaccine. J. Immunol. 172 (9), 5200–5205.

Martins Jr., M., S.F., Vilela, M., 2007. Multiscale models for the growth of avascular tumors. Phys.Life Rev. 4, 128–156.

Mattes, J., Hulett, M., Xie, W., Hogan, S., Rothenberg, M., Foster, P., Parish, C., 2003. Immunotherapy of cytotoxic T cell-resistant tumor by T helper 2 cells: an eotaxin and STAT6-dependent process. J. Exp. Med. 197 (3), 387–393.

Matzavinos, A., Chaplain, M., 2004. Travelling-wave analysis of a model of the immune response to cancer. C. R. Biol. 327 (11), 995–1008.

Matzavinos, A., Chaplain, M., Kuznetsov, V., 2004. Mathematical modelling of the spatio-temporal response of cytotoxic T-lymphocytes to a solid tumour. Math. Med. Biol. 21 (1), 1–34.

Nagy, J., 2005. The ecology and evolutionary biology of cancer: a review of mathematical models of necrosis and tumor cells diversity. Math. Biosci. Eng. 2 (2), 381–418.

Nishimura, T., Iwakabe, K., Sekimoto, M., Ohmi, Y., Yahata, T., Nakui, M., Sato, T., Habu, S., Tashiro, H., Sato, M., Ohta, A., 1999. Distinct role of antigen-specific T helper type 1 (Th1) and Th2 cells in tumor eradication in vivo. J. Exp. Med. 190 (5), 617–627.

Nonaka, M., Nonaka, R., Woolley, K., Adelroth, E., Miura, K., Okhawara, Y., Glibetic, M., Nakano, K., O'Byrne, P., Dolovich, J., Jordana, M., 1995. Distinct immunohistochemical localization of il-4 in human inflamed airway tissues. J. Immunol. 155, 3234–3244.

Ohnishi, H., Lin, K., Chu, T., 1990. Prolongation of serum half-life of interleukin-2 and augmentation of lymphokine-activated killer cell activity by pepstatin in mice. Cancer Res. 50, 1107–1112.

Ossendorp, F., Mengede, E., Camps, M., Filius, R., Melief, C., 1998. Specific T helper cell requirement for optimal induction of cytotoxic T lymphocytes against major histocompatibility complex class II negative tumors. J. Exp. Med. 187 (5), 693–702.

Owen, M., Sherratt, J., 1997. Pattern formation and spatiotemporal irregularity in a model for macrophage-tumour interactions. J. Theor. Biol. 189, 63–80.

Owen, M., Sherratt, J., 1998. Modeling the macrophage invasion of tumors: effects on growth and composition. Math. Med. Biol. 15, 165–185.

Owen, M., Sherratt, J., 1999. Mathematical modelling of macrophage dynamics in tumours. Math. Models Methods Appl. Sci. 9, 513–539.

Perez-Diez, A., Joncker, N., Choi, K., Chan, W., Anderson, C., Lantz, O., Matzinger, P., 2007. CD4 cells can be more efficient at tumor rejection than CD8 cells. Blood 109, 5346–5354.

Poe, M., Wu, J., Talento, A., Koo, G., 1996. Ctl lysis: there is a hyperbolic relation of killing rate to exocytosable granzyme a for highly cytotoxic murine cytotoxic t lymphocytes. J. Immunol. Methods 192, 37–41.

Qin, Z., Blankenstein, T., 2000. $CD4^+$ T cell-mediated tumor rejection involves inhibition of angiogenesis that is dependent of IFN-gamma receptor expression by nonhematopoietic cells. Immunity 12 (6), 677–686.

Regoes, R., Yates, A., Antia, R., 2007. Mathematical model of cytotoxic T-lymphocyte killing. Immunol. Cell Biol. 85 (4), 274–279.

Ribeiro, R., Mohri, H., Ho, D., Perelson, A., 2002. In vivo dynamics of T cell activation, proliferation, and death in HIV-1 infection: Why are $CD4^+$ but not $CD8^+$ T cells depleted? Proc. Natl. Acad. Sci. 99 15572–15577.

Roose, T., Chapman, S., Maini, P., 2007. Mathematical models of avascular tumor growth. SIAM Rev. 49 (2), 179–208.

Rosenberg, S., Lotze, M., 1986. Cancer immunotherapy using Interleukin-2 and Interleukin-2 activated lymphocytes. Annu. Rev. Immunol. 4, 681–709.

Sachs, R., Hlatky, L., Hahnfeldt, P., 2001. Simple ODE models of tumor growth and anti-angiogenics or radiataion treatment. Math. Comput. Modelling 33, 1297–1305.

Shankaran, V., Ikeda, H., Bruce, A., White, J., Swanson, P., Old, L., Schreiber, R., 2001. IFN-gamma and lymphocytes prevent primary tumor development and shape tumor immunogenicity. Nature 410 (6832), 1107–1111.

Slifka, M., Rodriguez, F., Whitton, J., 1999. Rapid on/off cycling of cytokine production by virus-specific cd8textsuperscript+ t cells. Nature 401, 76–79.

Smyth, M., Godfrey, D., Trapani, J., 2001. A fresh look at tumor immunosurveillance and immunotherapy. Nat. Immunol. 2 (4), 293–299.

Spratt, J., von Fournier, D., Spratt, J., Weber, E., 1993. Decelerating growth and human breast cancer. Cancer 71 (6), 2013–2019.

Spry, C., 1971. Mechanism of eosinophilia. VI. Eosinophil mobilization. Cell. Proliferation 4, 365–374.

Szymanska, Z., 2003. Analysis of immunotherapy models in the context of cancer dynamics. Int. J. Appl. Math. Comput. Sci. 13, 407–418.

Tepper, R., Coffman, R., Leder, P., 1992. An eosinophil-dependent mechanism for the antitumor effect of interleukin-4. Science 257, 548–551.

Toes, R., Ossendorp, F., Offringa, R., Melief, C., 1999. CD4 T cells and their role in atitumor immune responses [comment]. J. Exp. Med. 189 (5), 753–756.

Tracey, K., Cerami, A., 1994. Tumor necrosis factor: a pleiotropic cytokine and therapeutic target. Annu. Rev. Med. 45, 491–503.

van Gisbergen, K., Sanchez-Hernandez, M., Geijtenbeek, T., van Kooyk, Y., 2005. Neutrophils mediate immune modulation of dendritic cells through glycosylation-dependent interactions between mac-1 and dc-sign. J. Exp. Med. 201, 1281–1292.

Volpert, O., Foch, T., Koch, A., Peterson, J., Waltenbaugh, C., Tepper, R., Bouck, N., 1998. Inhibition of angiogenesis by interleukin 4. J. Exp. Med. 188 (6), 1039–1046.

Wan, Y., Bramson, J., Pilon, A., Zhu, Q., Gauldie, J., 2000. Genetically modified dendritic cells prime autoreactive T cells through a pathway independent of CD40L and interleukin 12: implications for cancer vaccines. Cancer Res. 60 (12), 3247–3253.

Yamagughi, Y., Hayashi, Y., Sugama, Y., Miura, Y., Kasahara, T., Kitamura, S., Torisu, M., Mita, S., Tominaga, A., Takatsu, K., Suda, T., 1988. Highly purified murine interleukin 5 (IL-5) stimulates eosinophil function and prolongs in vitro survival. J. Exp. Med. 167, 1737–1742.

Yates, A., Bergmann, C., van Hemmen, J., Stark, J., Callard, R., 2000. Cytokine-modulated regulation of helper T cell population. J. Theor. Biol. 206, 539–560.

Zeng, G., 2001. MHC class-II restricted tumor antigens recognized by $CD4^+$ T cells: new strategies for cancer vaccine design. J. Immunother. 24 (3), 195–204.

Zhang, S., Bernard, D., Khan, W., Kaplan, M., Bramson, J., Wan, Y., 2009. $CD4^+$ T-cell-mediated anti-tumor immunity can be uncoupled from autoimmunity via the STAT4/STAT6 signaling axis. Eur. J. Immunol. 39, 1252–1259.